SIMULATION OF DROPLET BREAKUP USING A LATTICE BOLTZMANN METHOD

F. R. Phelan Jr. and N. S. Martys
Polymers Division and Building and Fire
National Institute of Standard and Technology
Gaithersburg, MD 20899

Abstract

Droplet breakup in homogeneous shear flow at super critical Capillary numbers and a viscosity ratio of unity is studied using a lattice Boltzmann method. We find that the total number of child drops that form from an isolated super critical drop scales according to a power law relation (n = 3.5). The child drops that form are all below critical, but not wholly uniform in size, and the distribution appears to be log-normal at high drop numbers. It is also found that for large ratios of the Capillary number to its critical value, the total strain required to break up a drop into N sub-critical entities tends to a constant value.

Introduction

Taylor [1,2] determined that the behavior of droplets of equal density suspended in flow depends on the Capillary number

$$Ca = \frac{\eta_s \dot{\gamma} R}{\sigma} \tag{1.1}$$

and the viscosity ratio

$$M = \frac{\eta_d}{\eta_s} \tag{1.2}$$

where R is the drop radius, $\dot{\gamma}$ is the shear rate, σ is the surface tension, η_d is the drop viscosity and η_s is the viscosity of the suspending fluid. The Taylor theory predicts that below a critical capillary number, the drops will deform into ellipsoids whose shape is given by

$$\frac{L-B}{L+B} = Ca \cdot \frac{19M+16}{16(M+1)} \tag{1.3}$$

-- where L is the length of the drop, and B is the breadth -- and that above critical, the drops become unstable and break up into smaller, more stable entities whose capillary numbers are all below critical [3].

The behavior of super critical droplets, i.e., droplets whose capillary number exceeds the critical value, is of importance in a variety of fluid mechanics problems, and there is a generic interest in predicting the evolution of the second phase droplets during flow. Our interest is motivated by the processing behavior of immiscible polymer blends. The microstructure of the second-phase droplets -- i.e., their size, shape, orientation -- changes significantly as the polymer flows. These changes affect both the flow properties of the blend, and the final mechanical and physical properties of a part molded from such polymers.

In this paper, we undertake a numerical investigation of the flow behavior of individual drops in super critical systems. A variety of methods are available for modeling such behavior, e.g., lattice Boltzmann (LB) methods [4-14,20], coarse-grained Ginzburg-Landau type models [15-16], and continuum surface force methods [17-19]. We investigate three-dimensional drop breakup in homogeneous shear flow using the multi-component LB model of Shan and Chen [6-7,11]. As a starting point in our study, we consider the case of isolated drops. This was accomplished by using meshes with channel lengths (in the flow direction) long enough interactions between neighboring drop breakup families were eliminated. Our goal is to establish proper scaling relationships between the initial super critical capillary number, and the number of child drops that form, the distribution of drop sizes, and the rate at which the drop breakup occurs. Such relationships are necessary in order to characterize complex flows, where large spatial gradients in the shear rate (and hence the microstructure) are present.

Numerical Modeling

Lattice Boltzmann Method

The basic approach in the LB method is to solve the discrete Boltzmann equation for the particle velocity distribution function on a lattice. In the multi-component formulation, the particle velocity distribution function is denoted as $n_i^j(\underline{x},t)$ where the *i* subscript refers to components of the discrete velocity directions e_i, and the superscript *j* labels the fluid component.

Physically, the particle velocity distribution function indicates the quantity of particles at position $\underline{x}$ and time *t* for a given fluid component *j* which are traveling in the direction e_i. The traditional fluid flow quantities such as density and velocity for each component are obtained through the moment sums

$$\rho^j = m^j \sum_{i=1}^{N} n_i^j(\underline{x},t) \qquad (1.4)$$

$$\underline{u}^j = \frac{m^j}{\rho^j(\underline{x},t)} \sum_{i=1}^{N} e_i n_i^j(\underline{x},t) \qquad (1.5)$$

where $\rho^j(\underline{x},t)$ and $\underline{u}^j(\underline{x},t)$ are the macroscopic fluid density and velocity, m^j is the mass of fluid, and *N* is the number of velocities comprising the velocity space.

The evolution of the particle distribution function $n_i^j(\underline{x},t)$ is governed by the discrete Boltzmann equation given by

$$n_i^j(\underline{x}+e_i,t+1) = n_i^j(\underline{x},t) + \delta_i^j(\underline{x},t) \qquad (1.6)$$

where $\delta_i^j(\underline{x},t)$ is the collision operator which couples the set of velocity states, and the problem is scaled such that the time step is unity. The linear "BGK" form [4-5] of the collision operator is employed in which the distribution function is expanded about its equilibrium value

$$\delta_i^j(\underline{x},t) = -\frac{n_i^j(\underline{x},t) - n_i^{j(eq)}(\underline{x},t)}{\tau^j} \qquad (1.7)$$

where $n_i^{j(eq)}(\underline{x},t)$ is called the equilibrium distribution function and τ^j is a relaxation time for collisions controlling the rate of approach to equilibrium. The form of the equilibrium distribution function depends on the particular lattice model chosen. The three-dimensional, "D3Q19" model [9] which resides on a cubic lattice is used here (D3 indicates the model is three-dimensional, Q19 refers to the number of components in the velocity space).

To model phase-separation using the LB method, an interaction potential which produces a separating force between fluid components is introduced. We use the phase-separation model of Shan and Chen [6-7] where the interaction force for each fluid component is given by

$$F^j = -n^j \sum_{k=1}^{M} \sum_{i=1}^{N} G_i^{jk} n_i^k(\underline{x}+e_i) e_i \qquad (1.8)$$

where G_i^{jk} are fluid interaction parameters. The interaction force is introduced directly into the body-force term of the Boltzmann equation according to the procedure outlined in [11]. The Shan-Chen phase separation model produces an artificial surface tension that drives phase separation proportional to the local curvature of the interface boundary between two fluids [12].

SIMULATION

Flow Geometry and Boundary Conditions

Simulations were carried out for a two-component system consisting of a single isolated droplet in steady, homogeneous shear flow. The flow geometry and boundary conditions for the problem are shown in Figure 1. Periodic boundary conditions were used on the inlet, outlet, and side boundaries of the flow. The boundary conditions $\pm V_w$, where V_w is the wall velocity, were used on the upper and lower surfaces of the flow, respectively. As an initial condition, the droplet was placed at the center of the flow geometry as shown in Figure 2, with the entire system at rest.

The different values of the wall velocity and mesh sizes used in the simulations are shown in ***Table 1***, along with the corresponding values of the initial, super-critical capillary numbers. The critical capillary number for the system was determined to be 0.375, the first case shown in the Table. Because the boundary conditions at the inlet and outlet were periodic, it was necessary to lengthen the mesh in the flow direction as the capillary number went up, to prevent fluid exiting at the outlet and reentering at the inlet (and vice-versa) to coalesce upon itself.

General Observations

As expected, the simulation predicts that above the critical capillary number the drop stretches and breaks up into smaller entities. The simulations predict a three-stage mechanism for drop breakup. In the first stage, the drops are drawn into high aspect ratio liquid threads, with bulbous, "dumbbell" shaped ends. Once drawn, instabilities develop in the form of undulations in the cross-sectional area along the axis of the drop. In the final stage, the severity of the undulations causes child drops to pinch off from the ends of the main body until it is itself below the critical size.

The final configuration of some steady-state drop families for various capillary numbers are shown in Figures 3a-b. In this state, all the drops are stable, below the critical Capillary number. The drops are not uniform, there is a definite distribution of sizes. Table 2 gives the number of drops formed for each case, Table 3 breaks down the distribution of sizes. For the case of Ca = 0.9, we were not able to perform the calculations with a great enough mesh density to accurately resolve the great number of drops that form -- this will be an object of future work. We estimate the uncertainty of the data generated by the model to be 5%, based on the experience of the authors.

Number of Drops

Based on conservation of mass, we expect that there is some type of power-law relationship between N, the number of drops that form, and the initial super critical capillary number. Assuming that the family of child drops that form are well approximated by an equal average size, an approximate expression for the number drops that can be expected to form in super critical systems is

$$N = \frac{1}{\lambda^3}\left(\frac{Ca_0}{Ca_c}\right)^3 \qquad (1.9)$$

where λ is the ratio between the mean and critical drop size. Figure 4 shows that there is indeed a power law relation between N and the initial capillary number, but that the power law value is n = 3.5 (raw data values are given in Table 2). The difference in the exponent can be attributed to the distribution of sizes about the mean, where the distribution is skewed towards the small end.

Rate of Breakup

The strain required to break down the initial drop into N sub-critical entities is related to the rate at which the break-up process occurs. The strain to complete breakup as a function of Ca is plotted in Figure 5, where the strain is given by $\gamma = \frac{2V_w}{d}t$, and d is the distance between the upper and lower plate of our flow geometry. Beyond the simple cases of 2 and 3 drops, we find that the required strain appears to plateau at around a value of 38. This is an interesting result because it implies that for dilute systems in complex flows, drop breakup is complete in regions in which the critical strain has been reached.

Distribution

The drop size distribution for Ca = 0.75 are shown in Figure 6. There is a pronounced mean value, and as expected from the power-law relationship we observed between N and Ca, the number density is skewed towards the small end. This has the earmarks of a log-normal type distribution. However, subsequent studies at higher values of Ca are needed in order to reach a definitive conclusion.

Conclusion

Lattice Boltzmann simulations have been carried out for a two-component system in homogeneous shear flow at super critical Capillary numbers and a viscosity ratio of unity. The simulations predict a three-stage mechanism for drop breakup that is quite consistent with previous numerical work, and known experimental behavior. We find that the total number of child drops that form from a single isolated super critical drop scales according to the power law relation $N \sim (Ca_0)^{3.5}$. The child drops that form are all below critical, but not wholly uniform in size, and the distribution appears to be log-normal at high drop numbers. Also pertinent is the result that for large ratios of $\frac{Ca_0}{Ca_c}$ the total strain required to breakup the initial drop into N sub-critical entities tends to a constant value.

The present study has raised a number of questions we plan to address in future work. First, calculations at higher Ca are needed. This will allow us to further determine the range over which the observed power-law relationship between N and Ca is valid, and allow us to obtain enough drops to establish a valid statistical relation for the drop size distribution that is observed. A second issue we plan to address is the effect of coalescence. It can be expected that in non-isolated systems, drop-drop interactions will affect the results observed here.

References

1. Taylor, G.I., Proc. R Soc. Lond. A, 138, p. 41, (1932).
2. Taylor, G.I., Proc. R Soc. Lond. A, 146, p. 501, (1934).
3. Larson, R.G., The Structure and Rheology of Complex Fluids, Oxford University Press, New York, (1999).
4. Chen, H., Comp. Phys., 7, p. 632, (1993).
5. Hou, S., Lattice Boltzmann method for incompressible, viscous flow, Ph.D. thesis, Kansas State University, Manhattan, Kansas, (1995).
6. Shan, X. and Chen, H., Phys. Rev. E, 47, p. 1815, (1992).
7. Shan, X. and H. Chen, Phys. Rev. E, 49, p. 2941, (1994).
8. Shan, X. and Doolen, G., J. Stat. Phys., 81, p. 379, (1995).
9. Qian, Y.H., D'Humières, D., and Lallemand, P., Europhys. Lett., 1992, 17, p. 479, (1992).
10. Martys, N.S. and Chen, H., Phys. Rev. E, 53, p. 743, (1996).
11. Martys, N.S., X. Shan, and H. Chen, Phys. Rev. E, 58, p.6855, (1998)
12. Martys, N.S. and Douglas, J.F., Phys. Rev. E, 63, p. 031205-1, (2001).
13. Spaid, M.A.A. and F.R. Phelan Jr., Phys. Fluids, 9(9), p. 2468, (1997).
14. Spaid, M.A.A. and F.R. Phelan Jr., Composites A, 29A, p. 749, (1998).
15. R. Chella and J. Vinals, Phys. Rev. E, 53, p. 3832, (1996).
16. D. Jasnow and J. Vinals, Phys. Fluids A, 8, p. 660, (1996).
17. Brackbill, J.U., D.B. Kothe, and C. Zemach, J. Comp. Physics, 100, p. 335, (1992).
18. Zhang, D.F. and D.A. Zumbrennen, J. Fluids Eng., 118, p. 40, (1996).
19. Renardy, Y., V. Cristini, and J. Li, Int. J. Multiphase Flow, 28, p. 1125, (2002).
20. Xi, H. and C. Duncan, Phys. Rev. E., 59(3), p. 3022, (1999).

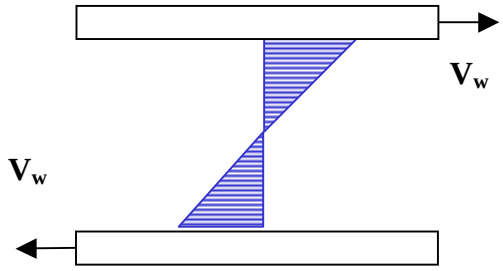

Figure 1 -- Unit cell and boundary conditions for homogeneous, shear flow. The upper walls move in opposite directions. Periodic boundary conditions are used at the inlet, outlet, and side boundaries of the flow.

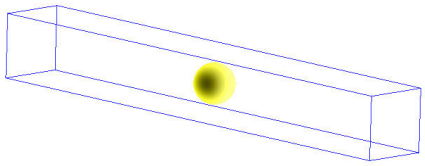

Figure 2 -- Initial condition for drop in steady, homogeneous shear flow. Upper and lower boundaries moved as indicated in Figure 1.

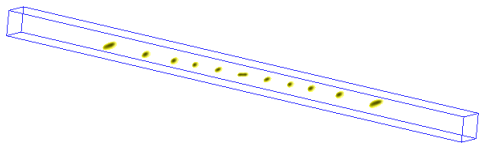

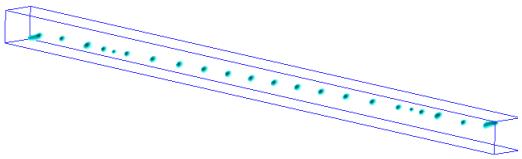

Figure 3a-c -- Steady-state drop families for Ca = 0.6 (top) and 0.75 (bottom), respectively.1

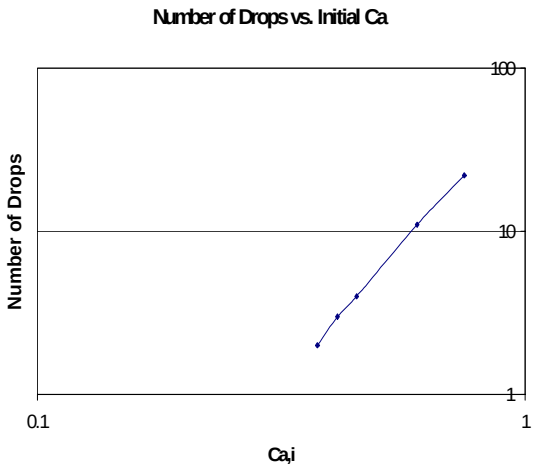

Figure 4 -- The number of drops that form upon breakup as a function of initial capillary number. The power law slope

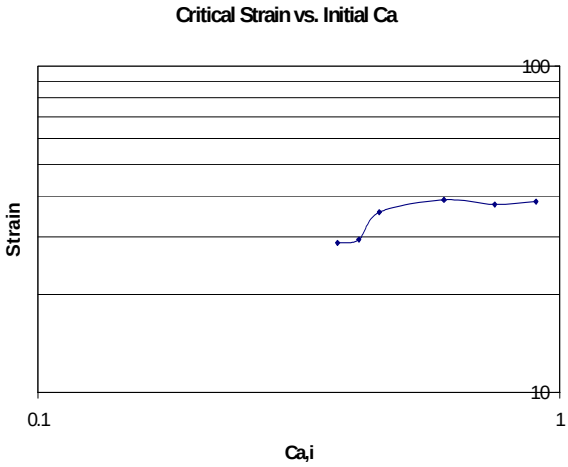

is 3.5.

Figure 5 -- The strain required to break up a into N sub-critical entities, as a function of initial capillary number.

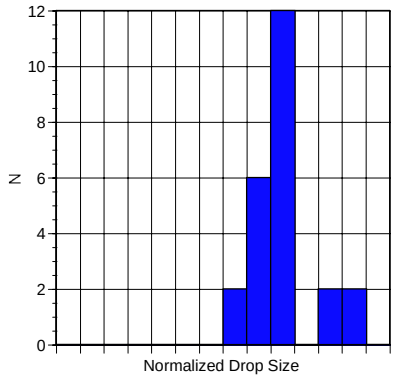

Figures 6 -- Drop distribution for the case of Ca = 0.75.

Wall Velocity (V_s)	Mesh Size	Initial Ca	Critical Diameter (D_c)
0.125	39 x 301 x 41	0.375	25
0.137	39 x 301 x 41	0.412	22.8
0.15	39 x 801 x 41	0.45	20.8
0.2	39 x 801 x 41	0.6	15.6
0.25	39 x 801 x 41	0.75	12.5
0.3	39 x 951 x 35	0.9	10.4

Table 1. Wall velocity (dimensionless) and mesh sizes used in the simulations. The initial capillary number of the drop and the critical diameter based on the wall velocity are also shown. The initial diameter of the drop is 25 mesh units in all cases. Longer meshes in the flow direction are needed as the initial capillary number is increased in order to wipe out the effects of periodicity.

Initial Ca	Number of Drops Formed	Strain to Breakup	Reduced Mean Diameter (D/D_c)
0.375	2	28.8	0.8
0.412	3	29.4	0.733
0.45	4	35.7	0.7
0.6	11	39.0	0.46
0.75	22	37.7	0.32
0.9	-	38.5	-

Table 2. The number of drops formed by shearing as a function of the initial super critical capillary number. No values are reported for the last case because the size of the smallest drops were too small to resolve for the given mesh cross-sectional density.

Initial Ca	Number of Drops	Drop Diameter	Reduced Diameter
0.375	2	20	0.8
0.412	1	17	0.68
	2	9	0.76
0.45	2	16	0.64
	2	19	0.76
0.6	4	10	0.4
	5	11	0.44
	2	15	0.6
0.75	2	6	0.24
	6	7	0.28
	12	8	0.32
	2	10	0.4
	2	11	0.44

Table 3. Drop distribution upon breakup for the different cases. The number of different discernable sizes broadens as the number of drops produced increases.